Groundwater recharge sources and mechanisms in the Ethiopian central Afar rift: insights from isotopic and hydrogeochemical tracers

Bereket Fentaw
bkrocks20@gmail.com
Addis Ababa University (AAU)
Behailu Birhanu
Addis Ababa University (AAU)
Tilahun Azagegn
Addis Ababa University (AAU)
Bekele Abebe
Addis Ababa University (AAU)

Research Article

Keywords: Deep groundwater recharge, NWP, Marginal graben, Afar rift

Posted Date: September 5th, 2023

DOI: https://doi.org/10.21203/rs.3.rs-3304107/v1

Additional Declarations: No competing interests reported.

Version of Record: A version of this preprint was published at Journal of African Earth Sciences on May 1st, 2024. See the published version at https://doi.org/10.1016/j.jafrearsci.2024.105299.

Abstract

The study of deep groundwater recharge and its flow pattern in a continental escarpment-rift interface zones is one of the most challenging subject in the field of hydrogeology. The central Afar rift and the associated western marginal grabens and Northwestern Plateau (NWP), in northeastern Ethiopia are an excellent examples, where the groundwater recharge and flow patterns are insufficiently addressed. Existing conceptual models argued on the existence of deep groundwater recharge to the rift, considering the marginal area as an overall barrier. But the role of interacting linking zones between the marginal grabens are commonly unaccounted for. Hydrogeochemical, stable isotopes of water and knowledge of geological structures are applied to determine groundwater recharge sources and mechanisms. There is a notable difference in isotopic compositions between the deep and shallow groundwater systems resulting from difference in recharge conditions. The major ion chemistry and EC of groundwaters in some corridors of western parts of the Afar rift show a clear geochemical evolution along the flow paths. The results of stable isotope and groundwater geochemistry revealed the existence of preferential deep groundwater recharge from the NWP, across the highly fractured linking zones, to the deeper volcanic aquifers of the central Afar rift. Overall, the groundwater flow from the NWP to the Afar rift is chiefly controlled by the orientations of the faulted marginal grabens and the linking zones between them. The suggested model of this study make a significant contribution to better understand groundwater recharge mechanisms in other similar continental rift zones.

Introduction

Within continental rift systems bounded by high mountains and steep escarpments, the possible recharge to the groundwater is believed to have two main sources: the first is recharge from surface flooding and perennial streams, and the second is deep groundwater inflow from the mountains (Kebede et al. 2007; Ayenewu et al. 2008 and references therein). The study of these groundwater recharge mechanisms is quite difficult because of the complex tectonic activities of the region, resulting in a discontinuous litho-stratigraphic setups and geomorphological features. This leads to a highly variable hydrogeological circumstances with discontinuous hydrostratigraphic units and a complex groundwater flow (Kebede et al. 2005; Bretzler et al. 2011; Yitbarek et al. 2012; Azagegn et al. 2015; Olaka et al. 2022).

Previous studies on the Ethiopian rift system tried to show that the dominant recharge source to the rift aquifers is deep groundwater flow from the mountain bounding the rifts (UNDP 1973; Craig et al. 1977; Darling et al. 1996; Chernet et al. 2001; Battistelli et al. 2002; Ayenew 2005). The existence of transverse structures crossing the rift system is likely supporting the groundwater recharge, channeled from the high mountains to the rift aquifers (Kebede et al 2007). Such phenomena has been clearly supported by the E-W trending structure of the Yerer Tullu Welel Volcanic Lineament (YTVL) (Kebede et al 2007; Agezegn et al 2015), which truncates the northern part of the Main Ethiopian Rift (MER). On the other hand, studies in central Afar and central Kenyan rifts suggested that deep groundwater inflow from the principal rift bounding high mountains to the rift floor aquifer is unlikely, rather localized recharge from streams is mainly responsible to recharge the aquifers of the rifts, (Kebede et al. 2007; Clarke et al. 1990). This has been explained by: the existence of typical graben and horst bounding structures at the interface between the Northwestern Plateau (NWP) and the Afar rift, together with the lack of transverse structures are acting as a barrier to the groundwater flow from the NWP to the rift aquifers (Kebede et al. 2007). However, the systematic arrangement of series of these marginal grabens connected by intensively cross-cutting faulted linking zones between them, and rift ward tilting faulted blocks (Abate et al. 1995; Acocella et al. 2000; Tesfaye et al. 2003; Tesfay 2005; Zwaan et al. 2020) may suggest the existence of hydraulic continuity between different aquifer systems, and hence deep groundwater recharge to the rift (Ayenew 2005; Mamo 2007; WEDSWS 20018). As a result, such areas can be recharged by a combination of the surface and subsurface origins.

Because of the highly variable spatial distribution of groundwater occurrence and complex recharge conditions, groundwater flow from the NWP and marginal grabens to the Afar rift has been a subject of arguments for at least two hypotheses. The first suggests that antithetic faults forming the western marginal grabens may assume to create closed and isolated hydrogeological systems separating it from the rift floor. The rift ward tilted blocks of tertiary flood basalt aquifers on the western margin may not continue till the inner rift fault. They are also assumed to be interrupted by chains of silicic volcanic ridges, which can hinder the cross-formation hydraulic conductivity continuities acting as a barrier for deep groundwater transfer from the western marginal graben area to the central Afar rift. This assumption has been evidenced by: (a) the nature of closed basins of the Hara and Hayk marginal grabens bounded by NNW-SSE antithetic faults to the east and N-S trending main rift bounding escarpment to the west, may imply isolated hydrogeological systems (ADSWE 2013). (b) A relatively modern and isotopically ($\delta^{18}O$ and $\delta^{2}H$) enriched signature of the groundwaters (shallow??) of the rift owning to recharge from evaporated surface water, suggests minimal or absence of deep groundwater recharge to the respective aquifers (Kebede et al. 2007). This assumption is also supported by the explanation, rifting proceeded by volcanism is the effect of deep rooted mantel upwelling in the Afar. This gives rise to the development of up doming and block forming faults and fractures, which further hindering groundwater circulation to the deep aquifers of the axial part of the rift (Tendaho graben) (GSE 2006).

The second assumption, suggests the existence of focused and litho-structurally controlled deep groundwater recharge from western marginal grabens and outer rift escarpment. This assumption includes the following possible evidences. (a) The N-S to NNW-SSE trending antithetic normal faults and the associated marginal grabens with an en-echelon arrangement are discontinuous along the western margin, and connected by multiple linking zones affected by intense faulting (Acocella, et al. 2000; Tesfay et al. 2003; Zwaan et al. 2020). These regions are supposed to contain overlapping damage zones (fractured zone on either side of faults) between each fault zones. Therefore, these regions are assumed to have greater permeability than the host rock and damage zones of each of these faults, serving as a path for deep groundwater flow from the western marginal area to the Afar rift floor. (b) The manifestation of thermal and old groundwaters as springs at the outlet of Raya graben near to Afar depression and at the linking zones between Raya and Hayk grabens (Fig. 1) (Mamo 2007; GSE 2015), and the existence of depleted isotopic composition in the deep groundwaters (250 to 500 m) of central Afar rift volcanic aquifers around Chifra and Elwuha areas (WEDSWS 2019). Now a days, the above two principal assumptions has been the center of scientific debate.

Previously, the role of interacting linking zones on deep groundwater recharge and flow from the NWP to the rift has been insufficiently addressed or may not accounted for. In this paper, the results of stable isotopes of water, EC, and geochemical tracer data from deep and shallow groundwaters and surface water together with previous geological knowledge at the interface between the NWP and central Afar rift are used. Recently, the increased density of deep well drilling (> 250 m) in previously uncounted areas particularly in the Afar rift gives us a better opportunity to understand the hydrogeochemical and isotopic signature of the deep aquifer system. By doing so, this study makes a significant contribution to deciphering deep groundwater recharge and flow from NWP to the deep volcanic aquifers of central Afar rift along preferential flow paths, giving special emphasis to the role of linking zones at the marginal area. The implication with regard to the relationship of groundwater dynamics within continental rift and mountains marked by the development of marginal grabens in between is also provided. Finally, based on the comparison of isotopic and hydrogeochemical compositions of the deep and shallow aquifer systems of the NWP and the rift with a specific emphasis to geological configuration of the marginal grabens, a new conceptual groundwater flow model is proposed.

The study area

The study area is located in the northeastern Ethiopia, and bonded by Latitude 12^0 56'and 11^0 02'N and longitude 39^0 20'and 41^0 45'E (Fig. 1).The elevation rages from 3500 m above sea level (a.s.l) on the western escarpment to 1200 m a.s.l in marginal grabens dropping to less than 300 m a.s.l on the rift floor. Most rivers including Borkena, Mile and

Awora draining the rift, begin from the bounding western mountains crossing the marginal grabens. Awash River is the dominant perennial river draining the rift floor following the Ethiopian rift structure. The formation of the Afar Depression and the associated escarpments are caused by two large-scale processes: the rotation of the Arabian plate with respect to the Nubian/African plate and the emplacement of a thermal mantle anomaly beneath the continental lithosphere (Ebinger and Sleep 1998; Beyene and Abduselam 2005; 2Bonini et al. 2005; Benoit et al. 2006; Furman et al. 2006; Acocilla et al. 2008; Zwaan et al. 2019 and 2020). The area is covered by a wide range of geological units from pre-rift tertiary volcanics, syn-rift volcanics and sediments, and recent volcanics and sediments (Barberi et al. 1975; Mohr 1983a; Tesfay et al. 2003; Wolfenden et al. 2005; Acocella et al. 2008, Alen eta al. 2017). The pre-rift (Oligocene) volcanics out cropped on the western escarpment of the rift and marginal grabens including numerous trap series volcanics which include basaltic and felsic lavas and pyroclastic deposits of Ashenge formations. While the syn-rift (Miocene-Pliocene) volcanics cover the western inner Afar rift extended up to marginal area of Tedaho graben, and comprised of silcic volcanic rocks of rhyolites, ignimbrites and/or trachytes, and the Pliocene-Pleistocene volcanic rocks of Afar stratoid basalts intercalated with fluvio-lacustrine sediments. The recent rift volcanics and sediments are outcropped in the rift axis and axial grabens, and includes quaternary rift axis rhyolite, early axial rift axis basalt, resent basaltic lava flows and Quaternary deposits of aeolian and alluvial sediments (Abate et al. 1995; Corti et al, 2015; Alen et al. 2017).

The current structural patterns are commonly quite complex and result from the interaction between the sub-aerial Red Sea and Aden rifts and the northern termination of the MER. The central Afar rift floor is dominantly characterized by NW-SE trending normal faults and more or less similarly oriented grabens of Tendaho and Dobi (Tesfay eta al. 2003; Tesfay 2005; Abebe et al. 2007; Keir et al. 2013; Corti et al. 2015). The N-S oriented western Afar margin is characterized by a series of NNW- SSE and N-S trending synthetic border faults and antithetic normal faults forming a right stepping en-echelon marginal grabens between them (Mohr 1983a; Wolfenden et al. 2005; Stab et al. 2016, Zwaan et al. 2020).

The major groundwater occurrence in the NWP is localized to the volcanic aquifers in intermountain valleys and shallow aquifers along streams. The static water level of wells on the Plateau and escarpment varies between 0 to 100 m b.l (below ground level) with a wide range of transmissivity from 0.2 to 340 m^2/day. Quaternary alluvial and thin lenses of lacustrine sediments comprise the major aquifer systems of the marginal grabens. The deep groundwater system of these grabens is also hosted in the underlying trap basalt aquifers. The transmissivity value in the marginal grabens shows a wide variation from 5 to more than 500 m^2/day. The depth to water level ranges from artisan type to not more than 50 m b.l.

The complex nature of the geological setup leads to the highly variable groundwater occurrence in the rift, where both thermal and cold groundwater manifestation can be observed on the axial parts. The aquifers in the rift comprise young quaternary basalts and alluvial/lacustrine sediments at shallow depth, at greater depth (>400 m) the main aquifer is dominated by Afar stratiod basalts interlayered with alluvio-lacustrine sediments. The groundwater of the rift is characterized by contrasting fresh and saline waters, where most of the fresh groundwater is localized near the Awash River and within the shallow quaternary basalt aquifers, it gets more saline away from the river. The water level for most deep wells in the Afar stratiod basalt varies between 39 to 121m b.l, however the value may reach up to 300 m b.l to the northeastern part. While for the shallow aquifers of alluvio-lacustrine sediments the range varies between 11 and 21 m b.l. Within the Tendaho graben, thermal spring water manifestations characterize the Alallobad and Dobi areas (Fig.1c). The main aquifers for these thermal waters are alluvio-lacustrine sediments and Afar stratiod basalts affected by cross-cutting deep faults. The transmissivity value in the western part of the rift floor around Chifra and Elwuha area is in the range of 55-430 m^2/day, while to the eastern part from Mile and Semera to Asayita area the

values increased to 750 m^2/day. The annual rainfall amount shows high variation from 1140 mm on the NWP to 150 mm on the rift floor.

Materials and Methods

Water samples were collected from boreholes, hand-dug wells, springs, rivers and lakes starting from February to March, 2017 and January to February, 2018. At each sampling sites p^H, electric conductivity (EC) and temperature were measured using portable OAKTON p^H and EC Tester30. Samples for major ions and stable isotopes (^{18}O & ^2H) were collected using 1L High-Density Polyethylene and 60 mL glass bottles respectively. A total of 114 water samples for stable isotope and major cations and anions have been collected. Out of these, three are from lakes, nine from rivers and the rest are from groundwaters. In addition, two rain-waters were sampled to understand the isotopic composition and major ion chemistry of rain-water in the region. The sampling for groundwater isotopic composition representation and geochemical analysis is done based on geomorphologic, lithologic and structural variation and recharge conditions.

The stable isotope analysis was carried out in the Isotope Hydrology Laboratory, School of Earth Sciences, Addis Ababa University. The measurements of stable isotope ratios in the water samples ($^1H/^2H$ and $^{16}O/^{18}O$) were done using the Liquid Water Stable Isotope Analyzer (LWIA), and converted to δ^2H and $\delta^{18}O$ compositions based on the Vienna Standard Mean Oceanic Water (VSMOW). The VSMOW is defined by the International Atomic Energy Agency (IAEA) from distilled sea water that was modified to have an isotopic compositions close to Standard Mean Oceanic Water (SMOW). This reference defines a value of $\delta = 0$. The results are reported as parts per million (‰). The analytical uncertainty in the measurement of stable isotope of water deuterium (δ^2H) and heavy oxygen ($\delta^{18}O$) using LWIA was reported to be ±2‰ for δ^2H and ±0.2‰ for ^{18}O. The measurements for major cations and anions were done in the Geosciences Laboratory Center of the Geological Survey of Ethiopia (GSE). The analytical methods used were titrimetry and spectrophotometry, and the results are presented in milligram per litter (mg/l). The results of stable isotope and physiochemical characteristics for selected water samples are presented in Table 1.

For a systematic analysis of the results, the area is divided to three major regions based on their hydrologic, geologic and geomorphologic setup, which are the Northwestern plateau (NWP), marginal area and the Afar rift (Fig. 2). The method for this study uses a comparative approach in stable isotope compositions variation and geochemical evolution of groundwaters crossways the above three regions, following Endumds et al. (2003) and Kebede et al. (2007). The technique can give capability to relate the groundwater interaction and flow between aquifers in escarpment-rift interface zones. By doing so the deep groundwater recharge and flow patterns can be addressed.

The record of isotopic composition from IAEA station of Addis Ababa rainfall from January 1965 to December 2009 was used to establish the Local Meteoric Water Line (LMWL), and to evaluate isotopic variations within the water bodies of the study area in view of the similarities in elevation of Addis Ababa area to that of northwestern escarpments. The weighted average isotope value for IAEA station at Addis Ababa summer rainfall (July and August) is -2.5 ‰ in $\delta^{18}O$ and -5.6 ‰ in δ^2H, and 15 in deuterium-excess (d-excess) and that of spring rainfall (March and April) is characterized by the values of 1.2 ‰ in $\delta^{18}O$ and 20 in δ^2H, and 10 in d-excess.

In addition, short term monitoring of Main Ethiopian Rift (MER) rainfall by Kebede (2004), and Desie town rainfall from IAEA GNIP (Global Network of Isotopes in Precipitation) project show a comparable isotopic composition and seasonal variation with Addis Ababa rainfall. Accordingly, for this study, an equation of a striate line $\delta^2H = 7.659\ \delta^{18}O + 11.8$ is found to represent the LMWL. The isotopic analysis of water samples collected from the study area are compared

relative to that of Addis Ababa rainfall monitored for long period of time, and to the isotopic compositions of local rainfalls of Desie and Chifra sampled during this study (Fig. 3).

Results and Discussions

Stable Isotope Composition of Oxygen ($\delta^{18}O$) and Hydrogen ($\delta^{2}H$)

The $\delta^{18}O$ and $\delta^{2}H$ contents in the groundwater and surface water of the region show a relatively wider range (Table 1 and Fig. 3). The isotopic compositions of all groundwaters from the NWP to the rift vary between -5.64 ‰ to 0.65 ‰ in $\delta^{18}O$ and -26.14 ‰ to 16.97 ‰ in ^{2}H‰ with an average value of -2.95 ‰ and -6.35 ‰ respectively. The river waters in the highlands and rift show similar isotopic compositions to the shallow groundwater systems, which range from -1.15 ‰ to 6 ‰ in $\delta^{18}O$ and -4.16 ‰ to 37.7 ‰ in $\delta^{2}H$. The lake waters are highly enriched in heavy isotopic compositions with values of 8.8 ‰ to 10.08 ‰ in $\delta^{18}O$ and 54.4 ‰ to 55.92 ‰ in $\delta^{2}H$.

Most groundwaters plot on the LMWL suggesting recharge from modern precipitation of the area (Fig. 3). From $\delta^{18}O$ - $\delta^{2}H$ plot, it is possible to observe that there is a clear distinction in isotopic compositions of deep and shallow groundwaters, where the deep groundwaters (>180m) from the three sectors plot to the depleted side of the graph (depletion in heavy isotopic composition), while shallow groundwaters (<150) are relatively enriched (Fig. 4). This clear segregation may not indicate a difference in sources of recharge rather the two systems have been recharged by the same sources (mountain rainfall), but under different mechanisms (Fig. 3, 4 and 9). The enrichment in shallow groundwater systems suggests that the aquifers have been subjected to mixing with evaporated surface water, hence most of the shallow water points are located near streams and flood plains. This can be also be supported by the evidence that most river waters plot on a similar position together with the shallow groundwaers, tend to shift slightly towards the evaporation line (Fig. 3 and 4). Besides, the depleted deep groundwater systems are recharged from the summer rain of NWP which undergo deep circulation without evaporation through volcanic aquifers (Fig. 4). Some high-yield cold springs and hot springs from the marginal grabens (at the interface between the mountain and the rift) are also depleted in $\delta^{18}O$ and $\delta^{2}H$ (Fig. 3), which have similar isotopic compositions with the deep groundwaters implying deep subsurface recharge from the NWP. Most low-yield springs and shallow wells plot together with the mountain summer rain testifying active and recent recharge from high land rainfall (Fig. 3).

Table 1. Chemical and stable isotope composition of all natural waters from the Northwestern Plateau (nwp), Marginal area (mg) and Afar rift (ar) (T = type of water samples, G = major geomorphologic group, s = shallow well, d = deep well, cs = cold spring, hs = hot spring, r = river, L = lake. The units are ‰ for δ^2H and $\delta^{18}O$, mg/l for major ions, µs/cm for EC and ^0C for temperature)

Sampling cod	locality	T	G	X	Y	p^H	EC	T^0	Na
sbh1	Arabati	s	mg	604368	1270769	7.07	776	27.5	37.4
sbh12	Hadar2	s	ar	626097	1240341	6.88	1926	31	197.5
sbh20	Meket1	s	nwp	497881	1295648	6.47	216	18	2.57
sbh28	Gobye	s	Mg	571027	1324402	7.78	619	25.7	28.80
sbh31	Bati1	s	mg	610511	1237620	7.29	827	24	56.90
sbh36	Gerado1	s	nwp	564708	1225536	7.82	419	23.2	20.30
sbh45	Girana2	s	Mg	580640	1278013	7.63	927	30.2	66.80
sbh46	Mesrsa1	s	mg	571830	1288141	7.66	497	23.9	16.6
sbh56	Woldia1	s	mg	563037	1306349	8.3	794	23.9	19.8
sbh82	Asayita4	s	ar	771981	1286112	7.91	2870	31.5	566
sbh84	Semera1	s	ar	726795	1307315	7.69	811	32.7	160.4
sbh86	Dubti	s	ar	725012	1298461	7.49	1430	33.3	269
dbh2	Chifra4	d	ar	611545	1283227	7.09	1081	33	54.8
dbh7	Elwuha1	d	ar	653294	1242275	7.37	1216	32.7	226.0
dbh8	Hadaar3	d	ar	666105	1233585	7.87	3350	34	659.5
dbh13	Desie1	d	nwp	566927	1238698	7.46	344	18	21.8
dbh17	Delanta1	d	nwp	517781	1282245	7.47	327	19.3	15.75
dbh40	Desie2	d	nwp	568979	1230036	7.84	659	20.6	32.5
dbh51	kombolcha3	d	mg	578907	1227572	8.04	676	22.4	35.9
dbh60	Hyke1	d	mg	573788	1248305	7.93	889	27.6	23.8
sbh62	Tenta1	d	nwp	523376	1238731	7.42	411	18.8	32.3
dbh81	Asayita3	d	ar	769587	1273517	7.63	5740	32.8	1139
dbh87	Logiya2	d	ar	747394	1280183	8.64	1782	34.7	360
dbh89	Mile2	d	ar	683799	1289428	7.94	1200	30.2	108
dbh91	Semera2	d	ar	718260	1304373	8.26	1216	29.8	253.3
csp1	Tewuledere	cs	mg	578323	1251602	7.03	636	27.5	25.5

csp5	Bokekisa1	cs	mg	597126	1264069	7.00	1698	26.4	100.0
csp8	Desie5	cs	nwp	552397	1223421	7.31	577	19.2	21.5
csp14	Debat	cs	nwp	545440	1319862	7.26	155	17.4	4.6
scp17	Dire Roka	cs	mg	593051	1296238	7.43	1203	26.1	82.0
csp18	Gidan	cs	nwp	540311	1321811	7.24	163	16.6	2.9
csp22	Mededo	cs	nwp	574139	1237782	7.68	357	18.3	15.1
csp35	Paso Mile	cs	mg	573848	1253840	7.45	672	23	33.2
csp36	Wurgesa	cs	mg	566550	1276454	7.78	639	24.6	20.1
csp39	Girana-chirity	cs	mg	578964	1277539	7.65	924	25.7	67.7
csp53	Tenta2	cs	nwp	517869	1254740	7.24	528	20.5	31
hsp1	Jari	hs	mg	571171	1255300	9.38	470	48.5	110.1
hsp2	Ambasel5	hs	mg	568631	1257949	8.23	412	48.4	81.6
hsp3	Alallobad	hs	ar	719524	1287975	7.8	2960	147	506.5
rw6	Mile at Jari	r	mg	569592	1257474	8.25	577	24.1	39.0
rw11	Borkena at Desie	r	nwp	570025	1228657	7.35	757	17.7	46.6
rw15	Mile at Mile	r	ar	692026	1261929	8.2	710	31.8	61.4
rw16	Awash at Asayita	r	ar	766812	1276796	8.8	812	34.2	140.9
lw1	Hayk	L	mg	575055	1253026	8.97	934	23.1	101.7
lw3	Afambo	L	ar	790426	1263837	9.71	7820	31.2	1828

Table 1 continued

	K	Ca	Mg	CO_2	HCO_3	Cl	F	SO_4	NO_3	SiO_2	^{18}O	^{2}H
sbh1	3.68	106.4	20.6		366.0	41.26	0.41	32.4	20.4	33.6	-1.64	2.72
sbh12	0.47	137.8	79.3		639.28	177.25	0.98	288.7	124.0	29.32	-0.11	5.46
sbh20	0.34	12.9	2.9		51.0	1.99	0.08	3.0	12.4	11.98	-1.91	-1.88
sbh28	0.31	59.7	26.4		325.74	17.8	0.18	20.5	21.26	34.35	-2.07	-0.28
sbh31	0.26	99.0	28.8		513.62	10.49	0.32	16.4	1.33	30.39	0.37	11.47
sbh36	2.74	52.8	11.2		248.88	7.8	0.18	5.53	4.43	0.17	2.52	15.03
sbh45	5.91	61.9	48.2		583.16	24.11	0.42	44.48	0.1	0.71	-1.66	-0.48
sbh46	0.90	36.1	20.1		249.0	8.51	0.24	13.04	4.43	0.35	-1.18	3.84
sbh56	1.07	78.9	40.7		414.8	29.07	0.26	21.98	18.16	0.74	-1.77	-1.64
sbh82	10.79	56.5	30.5	_	268	517.92	4.51	376	1.33	99.51	0.48	10.35
sbh84	7.45	12.2	8.5		231	99.26	3.55	97	1.77	38.95	-1.74	7.46
sbh86	3.32	30.3	30.5		374	170.87	1.83	147	3.99	29.53	0.65	3.19
dbh2	6.45	89.8	39.1	_	389.18	63.81	0.48	122.80	10.63	34.02	-4.72	-18.42
dbh7	3.03	39.0	22.0	_	206.0	138.0	0.66	75.0	487.3	29.1	-3.69	-13.99
dbh8	4.43	8.15	11.5	_	81.74	788.76	0.41	529.8	0.44	14.34	-3.58	-26.14
dbh13	0.64	38.00	12.7	_	190.32	5.67	0.1	10.30	13.29	18.4	-3.71	-10.12
dbh17	3.51	38.35	7.2	_	157.38	9.93	0.46	9.4	5.76	29.75	-3.72	-19.59
dbh40	1.95	74.5	18.6	_	305.0	34.74	0.2	19.78	18.16	1.1	-2.88	-10.45
dbh51	1.46	60.3	21.7	_	439.2	7.8	0.26	6.38	1.77	0.48	-3.32	-10.33
dbh60	2.31	64.8	21.4	_	372.1	8.15	0.27	14.15	2.22	0.32	-2.9	-12.04
dbh62	0.58	51.3	7.6	_	195.2	10.21	0.43	10.7	7.09	17.76	-3.97	-15.91
dbh81	9.36	118	108	_	561	808.26	2.12	1418.0	106.3	32.31	-3.85	-23.05
dbh87	10.5	<0.1	12	4.8	612.44	159.53	2.9	225.19	0.44	0.21	-4.23	-29.96
dbh89	2.5	48	55	_	280.6	78.7	0.53	221.44	7.59	196.9	-3.76	-23.41
dbh91	7.82	12	3.5	_	342.82	118.47	4.9	196.89	6.65	62.48	-4.45	-22.34
csp1	1.14	86.0	18.8		345.26	11.77	0.33	19.1	18.16	31.24	-1.79	-3.1
csp5	4.5	150.6	52.3		472.14	135.5	0.49	28.4	66.3	57.78	-1.88	-3.29
csp8	1.27	73.8	14.7		300.12	12.83	0.11	11.2	23.92	56.92	-2.75	-8.99
csp14	1.44	14.4	6.82		96.38	2.77	0.09	3.5	2.66	26.54	-4.28	-19.57
scp17	0.63	88.8	51.9		470.92	53.95	1.2	141.9	79.74	45.79	-1.71	2.64
csp18	0.92	17.1	7.9		100.04	0.78	0.1	3.3	5.32	28.67	-5.64	-18.83

csp22	1.13	42.6	11.7		195.26	4.18	0.1	5.9	13.29	31.67	-3.12	-3.43
csp35	3.2	84.8	17.2		305.0	21.13	0.41	23.0	44.3	0.68	-2.19	-1.03
csp36	0.53	73.3	45.1		414.8	16.31	0.31	34.1	13.29	0.48	-2.24	0.32
csp39	0.53	98.0	49.3		523.38	30.35	0.32	26.2	33.23	0.91	-2.47	-2.9
csp53	4.15	60.6	14.5		292.8	10.64	0.45	21.5	0.44	29.96	-2.14	-7.04
hsp1	1.11	3.1	0.5	45	157.38	14.18	2.64	13.99	0.1	0.52	-3.48	-16.39
hsp2	0.39	9.2	2.7	_	231.8	8.86	1.07	27.64	0.1	0.28	-2.52	-7.37
hsp3	34.5	20	4.5	22	45.14	570.75	1.4	306.05	0.89	211.9	-3.28	-27.3
rw6	1.04	66.9	19.3	_	341.6	10.64	0.36	20.7	0.1	46.2	-1.68	-1.46
rw11	9.17	74.2	20.5	_	305	56.72	0.33	16.15	20.37	34.6	-1.85	-4.16
rw15	4.2	22.4	29.2	_	268	22.8	1.8	45.7	2.9	44	0.8	3.9
rw16	9.2	20.3	6.7	_	351	71.1	2.4	48.8	8.8	47.5	6	37.7
lw1	12.59	19.2	63.9	60.0	423.0	50.34	0.99	11.4	0.1	1.7	9.07	54.77
lw3	26.68	49	15	482	2092.3	767.49	2.2	633.89	9.75	14.12	10.08	55.92

Awash River at Asayita show higher isotopic enrichment with values of 6 ‰ in $\delta^{18}O$ and 37.7 ‰ in $\delta^{2}H$ (Fig. 3 and Table 1), this could be related to isotopic enrichment in river evaporation due to the very slow flow of the river resulting from the flat topography of the area. Some groundwaters from hand dug wells and shallow wells along the river show similar isotopic enrichment plotting on the mixing area, suggesting the recharge of shallow aquifers by the Awash River (Fig. 3).

The thermal springs of Alallobad and some deep wells of the Afar rift characterized by a depleted $\delta^{2}H$ content, plot below the LMWL with a slight positive shift in $\delta^{18}O$ (Fig 3 and 4). A similar oxygen shift has been also observed further east near Lake Abhe thermal waters in Djibouti (Giovanni et al. 1998; Housseina et al. 2013). This positive shift in $\delta^{18}O$ as suggested by UNDP (1973) and Kebede et al. (2007) is related to the ^{18}O exchange between the geothermal waters and the silicate rock matrix of the reservoir. The depletion in $\delta^{2}H$ is also suggested as different recharge origin, as compared to the shallow aquifers, under colder climate conditions, which is subsurface recharge from the NWP (UNDP 1973; Battistelli et al. 2002). Besides, the isotopic signature of recently drilled (WEDSWS 2019) deep wells (dbh2 & dbh8) at the western part of the rift floor around Chifar and Elwuha areas show significant depletion in $\delta^{18}O$ and $\delta^{2}H$ with values range from -4.7 ‰ to -3.88 ‰ in $\delta^{18}O$ and -23.14 ‰ to -18.42 ‰ in $\delta^{2}H$ (Table1), suggesting the existence of subsurface recharge to the deep volcanic aquifers of the western parts of the rift from the heavy summer rainfall that falls on the NWP. Such evidence has been also observed further east to some localities of Semera-Logiya (dbh87 and dbh91) at the axial part of the rift particularly in the Tendaho graben, which could result from regional lateral groundwater flow along the axial part of the rift. Similar lateral groundwater flows are also documented at the MER (Kebede et al. 2007; Hailu et al. 2023).

In Fig. 5, the spatial variation of $\delta^{18}O$ and $\delta^{2}H$ of groundwters from the NWP across marginal garbens to the rift show significant distinctions, where there is both depletion and enrichment. In all the three regions, there are two systems manifested by distinct isotopic compositions, where the shallow aquifer system showing a progressive enrichment towards the rift suggesting the importance of evaporative fractionated water infiltration from flesh floods and stream

channel loss to the shallow aquifers of the rift. The deep aquifer systems in the rift and the marginal grabens have low contents of $\delta^{18}O$ and $\delta^{2}H$ similar to the NWP, suggesting deep groundwater connection between them.

Electric Conductivity (EC) and Major ion chemistry

The pH values range from slightly neutral to alkaline (6.47 –9.38) in the groundwaters. Temperatures in geothermal influenced areas exceeded 100°C and EC reached values over 5000 µS/cm with a range of 143 µS/cm in cold springs from the NWP to 5740 µS/cm in deep well from the rift. In general, higher pH (> 8), EC and water temperatures were found in the groundwater of the rift floor compared to the higher escarpments. The progressive increase in groundwater temperature from the escarpment to the rift corresponds to the increase in ambient air temperature and the increase in geothermal gradient. Surface water samples have a wide range of EC, with lower values measured in the rivers (195 – 812 µS/cm) and the highest EC values of >7000 µS/cm found in the alkaline lake Afambo. Surface water temperatures are lower than that of groundwater, but their pH ranges are similar.

The dominant cation in the groundwaters of NWP is Ca followed by Na and Mg, while in the rift and marginal areas Na is the dominant followed by Ca (Fig. 6a-c). In the marginal area, a significant proportion of Mg existed as compared to the rift (Fig. 6b). The dominant anion measured on the groundwater of NWP and marginal gabens is HCO_3 followed by Cl, while in the rift Cl is dominant followed by comparable proportion of HCO_3 and SO_4 (Fig. 6a-c). Major ion compositions of river from the three sectors are the reflection of the respective groundwaters, except a relatively higher proportion of HCO_3 in the rift rivers (Fig. 6f). Lakes from marginal grabens are dominated by Mg and HCO_3 with a comparable Na content (Figure Lakes from marginal grabens are dominated by Mg and HCO_3 with a comparable Na content (Figure 3h). Na is by far the dominant cation in the Afar Lakes, and Cl is the dominant anion followed by HCO_3 (Fig. 6g). Nitrate concentration is low in most groundwaters and surface waters (< 10 mg/l). Higher values greater than 100 up 347.3 mg/l are observed in shallow wells and hand dug wells from marginal grabens and Afar rift (Fig. 5e and Table 1), resulted from anthropogenic sources specific to areas where there are agricultural activities.

Fig. 7a-c, it is possible to observe a rift ward progressive increase in Na, K, Ca, Mg, HOC_3, Cl and SO_4 concentrations in groundwaters from the NWP across marginal grabens to the rift. The water type shows variation from Ca and HCO_3 dominant type to Na and HCO_3 dominant in the marginal area to Na, Cl, and SO_4 dominant type in the rift. The significant HCO_3 content increase from the plateau to the marginal grabens is coherent with Kebede et al. (2007), indicating the importance of the hydrolysis reaction in imparting HCO_3 near the mountains. This increase of HCO_3 together with the exchange of Ca by Na content could suggest a groundwater connection between the aquifers of NWP and marginal grabens. There is no clear progressive increase in HCO_3 from marginal grabens to the rift particularly in the thermal groundwaters of Tendaho graben. For example, the HCO_3 content in the thermal springs of the Allalobad is very low, suggesting alkalinity loss related to the dissolution of lacustrine sediment and evaporites in the geothermal reservoirs (Kebede et al. 2007). On the other hand, few deep wells in the rift to the west of Tendaho graben are characterized by increased Na and HCO_3 dominant type (Fig. 8a and c). This incremental evolution of deep groundwater is also consistent with their depleted content of ^{18}O and $\delta^{2}H$.

The progressive increase in Cl and SO_4 in the axial part of the rift could be related to the heterogeneity in the aquifer system due to intensive structural and volcanic activities. In general, most groundwaters with high salinity in the Afar rift are related to geogenic sources of salt dissolution/interaction with the aquifer matrix (Fig. 8a-e).

Fig. 9 shows the relationship of EC with $\delta^{18}O$ of surface waters, and deep and shallow groundwater form NWP, marginal grabens and the rift. The graphs help to see recharge mechanisms and controlling geochemical and climatic process. Waters with high EC and depleted isotopic content recorded in the deep groundwaters of Afar and the thermal

springs of Alallobad are clearly differentiated from the rest of the groundwaters. Salt dissolution/interaction with the aquifer matrix along the flow path could be the dominant mechanism in these deep aquifer systems. Isotopic enrichment in ^{18}O with low to moderate EC was observed on the Lakes Hayk and Hardibo (from the marginal area), rives and some shallow wells from the Afar rift, indicating evaporation dominant system. Most deep wells, cold and hot springs from NWP and Marginal areas show low ^{18}O and low to moderate EC affirming fresh active groundwater recharge from the mountains (Fig. 9a and b). While most shallow aquifers on the marginal grabens and the rift plot in between, on the mixing line/processes. Extremely high EC and high ^{18}O content observed in the Lake Afambo from Afar rift indicate peculiarity, reflecting a high degree of evaporation from the lake surface accompanied by significant mixing contribution with groundwaters, which undergo salt dissolution.

Groundwater recharge the role of NWP and marginal grabens

Results of the stable isotopes of oxygen and hydrogen and groundwater geochemistry provide valuable information on the recharge origin and mechanisms. The variation in stable isotopes ($\delta^{18}O$ and $\delta^{2}H$) in the groundwaters indicates difference in recharge origin. The progressive increase in major ion and EC of groundwaters from the escarpment to the rift is dominantly the result of heterogeneity of the aquifers matrix, however in some corridors of the marginal grabens and western parts of the rift a clear geochemical evolution along the flow line can be observed. In this study, the results of stable isotope and groundwater geochemistry revealed the following different modes of groundwater recharge:

1. Direct recharge from moderen precipitations on the escarpment and marginal grabens. Groundwaters in the escarpments are mostly depleted in the heavy isotopes of hydrogen and oxygen with low contents of major ions and EC, similar to rainfall, indicating their direct recharge relationship. These recharge types are also observed in the marginal grabens and horsts resulting from quick infiltration recharge, mainly along permeable fault fractures at the foot of the escarpment, and direct infiltration in sediments filling the grabens. Such groundwater recharge often resulted in the manifestation of springs and artesian wells at the marginal grabens around Hayk-Girana area.

2. Recharge from flash flood, stream channel loss and the Awash River, which is mainly observed in the shallow aquifers of the rift floor. A relatively enriched groundwater and moderate EC of this types are the results of evaporation before recharge. Most small streams and groundwater discharged as springs at the marginal grabens joined to form major streams (for example: Mile and Logiya), and undergo evaporation while flowing to the rift before recharging the shallow aquifers of the Afar rift floor. Such kind of recharge mode is also outlined by Ayenew et al. (2005) and Kebede et al. (2007). The rift floor shows variable water type from dilute to concentrate due to geogenic enrichment. This could be related to the diverse lithological types and structural setup, including previously weathered and deposited alluvio-lacustrine, and evaporites intervening with faulted and fractured basaltic and silcic volcanic rocks.

3. Deep subsurface recharge from NWP through selected structurally controlled paths, along Woldia-Chifra, and Kombolcha-Bati-Elwuha tracts. This mode of recharge can be evidenced by hot springs and deep groundwaters of volcanic aquifers from the marginal grabens and Afar rift floor, characterized by low contents of ^{18}O and $\delta^{2}H$ and high EC (Fig. 4, 5 and 9), which makes it distinct from the shallow systems of the rift implying dissimilarity in recharge mechanisms. This groundwater flow pattern is preferential, and highly controlled by fault systems on the marginal grabens and horsts. The N-S to NNW-SSE trending antithetic normal faults and associated marginal grabens are discontinuous with en-echelon arrangement (Fig. 1) along the western margin, connected by multiple linking zones, which in turn affected by intense fracturing (Tesfaye et al. 2003). These regions containing overlapping linking damage zones (fractured zone on either side of faults) between each fault zone, with greater permeability than the host rock and damage zones of each of these faults is serving as preferred paths for deep groundwater flow from the western marginal area to the Afar rift floor.

Largely, the results of this study is supporting the existence of preferential deep groundwater recharge from NWP and western marginal area to the rift floor. Therefore, the marginal grabens may not have an overall barrier role for the regional groundwater flow to the rift.

Conceptual model of groundwater flow

The groundwater flow and recharge mechanisms of the region is remarkably highly controlled by the architecture of the marginal and the rift structures. The groundwater in the rift floor is separated in to two distinct systems of deep and shallow aquifers with different recharge mechanisms. The deep aquifer systems are recharged by a deep preferential groundwater flow from NWP (Fig. 10b) owning to the existence of structurally interacting zones in between the marginal grabens. The shallow aquifers of alluvio-lacustrine sediments and recent basalts are predominantly recharged by surface flooding and stream channel loos. In the volcanic aquifers of marginal graben of Hayk, there is also a deep groundwater flow from the NWP. Shallow and local groundwater flows are responsible in recharging the alluvial aquifers of the marginal grabens and the rift floor (Fig. 10b).

In the western part of rift floor (Chifra and Elwuha area), it is very unlikely that the shallow groundwaters mix with the deep groundwater systems. However, in some localities of the eastern part around Alallobad the lateral shallow groundwater flow is mixing with the deep system rising as thermal springs, which attests the role of boarder faults of Tedaho graben. Within the fracture zones of marginal area, it is also possible to point out that the deep groundwaters are raising to the shallow aquifers, and manifesting as hot springs owning to the interacting fractures in between the Hayke and Raya grabens.

The geochemical evolution of groundwater at the interface between the NWP and marginal area involves silicate mineral weathering/dissolution, with a progressive increase in major ions and EC towards the marginal area. In the rift floor the groundwater geochemical increment is attributed to multiple factors, from dissolution of alkaline rich basalts and evaporites found in lacustrine sediments to the effects of hydrothermal and volcanic activities as well as mixing between evaporated surface water and shallow aquifers.

Conclusions

Stable isotope compositions and major ion chemistry as well as previous geological knowledge are used to investigate groundwater recharge sources, mechanisms and flow pattern at the interface between the NWP and Afar rift of Ethiopia. The study points out that the understanding of groundwater recharge and flow in this continental rift zone, dominantly depend on the tectonic structures that complicate the hydrogeological properties of aquifers. In this study, two main possible groundwater recharges in the marginal grabens and the rift floor are identified. The first is recharge from flash flood and through the Awash River. Heavy flooding from the NWP during the rainy season, and the streams and springs discharged at the marginal grabens, which later join to form major rivers flowing to the rift, are recharging the shallow aquifers of the Afar rift floor. The second is a preferential deep groundwater recharge from the NWP and marginal grabens in to the deep aquifer systems of the rift. This type of flow is highly controlled by the orientation of marginal grabens and the faults which form them, where the marginal grabens are discontinuous with an en-echelon arrangement connected by multiple linking zones affected by intense fracturing. This work identified that these regions of relay ramps as important structural features that provide a mechanism for lateral continuity of geologic/aquifer units, and therefore mediate groundwater flow from the high-elevation western escarpment recharge area to the rift floor. The study observed, such phenomena, particularly along Woldia-Chifra, and Kombolcha-Bati-Elwuha tracts.

The progressive increase in EC and major ion chemistry in the axial parts of the rift are dominantly the result of heterogeneity in the aquifer systems due to intensive structural and volcanic activities. However, some clear

geochemical evolutions along the flow path from the western escarpment to the rift are observed, and represented by a progressive increment of HCO_3 and Na in the deep aquifer systems of marginal grabens and western part of the Afar rift floor (Chifra-Elwuah-Mile area).

Most of the salinity sources in the region are the results of geogenic process/salt dissolution and high evaporation from surface water and shallow aquifers in the rift floor. However, some high NO_3 pollution observed near farm-lands within the marginal garbens and the rift are the result of anthropogenic sources from farming activities.

Groundwater dynamics in the interface zone of the NWP and Afar rift is highly influenced by the complex set-up of the marginal and axial structures. Therefore, further groundwater recharge origin and dynamic studies should focus on an integration of isotope and geochemical tracer methods together with a direct geological structural investigations across the marginal and axial grabens, particularly in the Tendaho graben.

Declarations

Acknowledgments This work is part of the International Atomic Energy Agency Technical Cooperation Projects (ETH 7006 and ETH 2001204) conducted in collaboration with the Geological Survey of Ethiopia (GSE) and Addis Ababa University (AAU).

Author contributions All authors have contributed for the manuscript equally

Conflict of interest The authors declare that they have no conflict of interest

References

1. Abate E, Pietro PP, Leonardo ZL (1995) A strike-slip faults in a rift area: a Transect in the Afar triangle, East Africa. Tectonophysics 241 (1995) 67-97
2. Abebe B, Acocella V, Korme K, Ayalew D (2007) Quaternary faulting and volcanism in the Main Ethiopian Rift. J Afr Earth Sci 48 (2007) 115–124
3. Acocella V, Gudmundsson A, Funiciello R (2000) Interaction and linkage of extension fractures and normal faults: examples from the rift zone of Iceland. J Struct Geol 22 (2000) 1233–1246
4. Acocella V, Abebe B, Korme T, Barberi F (2008) Structure of Tendaho Graben and Manda Hararo Rift: implications for the evolution of the southern Red Sea propagator in Central Afar. Tectonics 27: TC4016. http://dx.doi.org/10.1029/2007TC002236
5. ADSWE (2013) Groundwater potential assessment of Eastern Amhara development corridor of Awash Basin (Kobo-Robit-Minjar) Project. Groundwater potential evaluation report. Amhara Design and Supervision Works Enterprise resource, Bahir Dar, Ethiopia
6. Alene M, Hart WK, Saylor BZ, Deino A, Mertzman S, Haile-Selassie Y, Gibert LB (2017) Geochemistry of Woranso-Mille Pliocene Basalts from West-Central Afar, Ethiopia: Implications for mantle source characteristics and rift evolution. LITHOS doi:10.1016/j.lithos.2017.03.005
7. Ayenew T (2005) Major ions composition of the groundwater and surface water systems and their geological and geochemical controls in the Ethiopian volcanic terrain. SINET: Ethiopian J Sci 28:171–188
8. Ayenew T, Demlie M, Wohnlich S (2008) Hydrogeological framework and occurrence of groundwater in the Ethiopian aquifers. J Afr Earth Sci 52 (2008) 97–113
9. Azagegn T, Asrat A, Ayenew T, Kebede S (2015) Litho-Structural control on inter-basin groundwater transfer in Central Ethiopia. J Afr Earth Sci 101 (2015) 383-395

10. Barberi F, Ferrara G, Santacroce R, Varet J, (1975) Structural evolution of the Afar Triple Junction: In Afar Depression of Ethiopia. 1 Schweizerbart, edited by A. Pilger and A. Rösler, 38–54. Stuttgart, Germany: E. Schweizerbart'sche Verlagsbuchhandlung
11. Battistelli A, Yiheyi A, Calor C, Ferragina C, Abatneh W (2002) Reservoir engineering assessment of Dubti geothermal field, Northern Tendaho Rift, Ethiopia. Geothermics 31:381–406
12. Benoit M, Nyblade A, VanDecar J (2006) Upper mantle P wave speed variations beneath Ethiopia and the origin of the Afar hotspot. Geology 34:329–332
13. Beyene A, Abduselam MG (2005) Tectonics of Afar Depression: A review and synthesis. J Afr Earth Sci 41 (2005) 41–59. doi: 10.1016/j.jafrearsci.2005.03.003.
14. Bonini M, Corti G, Innocenti F, Manetti P, Mazzarini F, Abebe T, Pecskay Z (2005) Evolution of Main Ethiopian Rift in the frame of Afar and Kenya rift propagation. Tectonics 24, TC1007. https://doi:10.1029/2004TC001680, 2005
15. Bretzler A, Osenbrück K, Gloaguen R, Ruprecht J , Kebede S, Stadler S (2011) Groundwater origin and flow dynamics in active rift systems: A multi-isotope approach in the Main Ethiopian Rift. J Hydrol 402(3–4), 274–289. https://doi.org/10.1016/j. jhydrol.2011.03.022
16. Chernet T, Travi, Y, Valles V (2001) Mechanism of degradation of the quality of natural water in the lakes region of the Ethiopian Rift Valley. Water Res 35:2819–2832
17. Clarke MG, Woodhall DG, Allen D, Darling G (1990) Geological, volcanological and hydrogeological controls on the occurrence of geothermal activity in the area surrounding lake Naivasha, Kenya. Ministry of Energy Report
18. Corti G, Bastow ID, Keir D, Pagli C, Baker E (2015) Rift-related morphology of the Afar Depression. World Geomorphological Landscapes. https://doi 10.1007/978-94-017-8026-1_15
19. Craig H, Lupton JE, Horowiff RM (1977) Isotope geochemistry and hydrology of geothermal waters in the Ethiopian Rift Valley. Report no. 160, Scripps Institute of Oceanography, University of California, San Diego, CA
20. Darling G, Gizaw B, Arusei M (1996) Lake-groundwater relationships and fluid-rock interaction in the East African Rift Valley: isotopic evidence. J Afr Earth Sci 22:423–430
21. Ebinger C and Sleep NH (1998) Cenozoic magmatism in central and east Africa resulting from impact of one large plume. Nature 395:788–791
22. Enmunds WM, Guendouz AH, Mamou A, Moulla A, Shand P, Zouari K (2003) Groundwater evolution in the Continental Intercalaire aquifr of south Algeria and Tunisia: Trace element and isotopic indicators. Appl Geochem 18:805-822.
23. Furman T, Bryce J, Hanan B, Yirgu G, Ayalew D (2006) Heads and tails: 30 years of the Afar plume. In:Yirgu G, Ebinger CJ, Maguire PKH (eds) The Afar volcanic province within the East African Rift System. Geol Soc Lond Spec Publ 259:95–119
24. Giovanni G, Negussie M, Stefano B, Alessandro C, Paolo G, Giovanni R, Mirco M, Zewde G (1998) Water–rock interaction and hydrothermal mineral equilibria in the Tendaho Geothermal System. J Volcanol Geotherm Res 86 (1–4): 253–276
25. GSE (2006) Geological, surface hydrothermal alteration and geothermal mapping of Dubti-Semera area, Tendaho Geothermal Field. Unpublished report. Geological Survey of Ethiopa, Addis Ababa.
26. GSE (2015) Consultancy services for geothermal surface exploration in Tendaho Alalobeda, Ethiopia Geochemical Report. Unpublished report, Geological Survey of Ethiopia, Addis Ababa.
27. Hailu K, Birhanu B, Azagegn A, Kebede S (2023) Regional groundwater flow system characterization of volcanic aquifers in Upper Awash using multiple approaches, central Ethiopia. Isotopes in Environmental and health studies. dio:10.1080/10256016.2023.2222221

28. Hussein B, Chandrasekharam D, Chandrasekharc V, Jalludina M (2013) Geochemistry of thermal springs around Lake Abhe Western Djibouti. Int. J. Sustain. Energ. doi:10.1080/14786451.2013.813027.
29. Kebede S (2004) Approches isotopique et geochimique pour l'etude des eaux souterraines et des lacs: Exemples du haut bassin du Nil Bleu et du rift Ethiopien [Environmental isotopes and geochemistry in groundwater and lake hydrology: cases from the Blue Nile basin, main Ethiopian rift and Afar, Ethiopia], PhD Thesis, University of Avignon, France
30. Kebede S, Travi Y, Alemayehu T, Ayenew T (2005) Groundwater recharge, circulation and geochemical evolution in the source region of the Blue Nile River, Ethiopia. Appl Geochem 20:1658–1676
31. Kebede S, Travi Y, Asrat A, Alemayehu T, Ayenew T, Tessema Z (2007). Groundwater origin and flow along selected transects in Ethiopian rift volcanic aquifers. Hydrogeol J 16, 55-77. https://dio:10.1007/s10040-007-0210-0
32. Keir D, Bastow I, Pagli C, Chambers E (2013) The development of extension and magmatism in the Red Sea rift of Afar. Tectonophysics 607:98–114
33. Mamo S, (2007). Hydrogeology, Hydrogeochemistry and Isotope hydrology of Raya and Kobo Valleys, Adjacent Plateau, Escarpment and Part of Afar Rift, Ethiopia: Hydrogeological mapping, recharge evaluation and water Quality assessment. Unpublished report, Geological Survey of Ethiopia, Addis Ababa
34. MOW (2009). Hydrogeological investigation report for Kobo-Girana pressurized irrigation project. Ministry of water resource, Addis Ababa, Ethiopia
35. Mohr PA (1983a). Prospective on Ethiopian province. Bull Volcanol 46-1
36. Olaka LA, Kasemann SA, Sültenfub J, Wilke FDH, Olago DO, Mulch A, Musolff A (2022). Tectonic control of groundwater recharge and flow in faulted volcanic aquifers. Water Resources Research, 58, e2022WR032016. https://doi. org/10.1029/2022WR032016
37. Stab M, Bellahsen N, Quicelleur X, Ayalew D, Leroy S (2016) Modes of rifting in magma- rich settings: Tectonomagmatic evolution of Central Afar. Tectonics, 35, 2-38. 1202 https://doi.org/10.1002/2015TC003893
38. Tesfaye S, Harding D, Kusky T (2003) Early continental breakup boundary and migration of the Afar triple junction, Ethiopia. Geol Soc Am Bull 115:1053–1067
39. Tesfaye S, (2005) Fault population investigation and estimating magnitude of extension in Guma Graben, Central Afar, Ethiopia. J Afr Earth Sci 41 (2005) 437–444
40. UNDP (1973) Geology, geochemistry and hydrology of hot springs of the East African Rift system within Ethiopia. UNDP report DD/SF/ON-11, UNDP, New York, 300 pp
41. WEDSWS (2018 Kobo Chefa groundwater resource evolution, assessment and test wells drilling supervision project: Groundwater potential assessment of Woldia-Tisabal Area. Ethiopian Construction Design and Supervision Works Corporation, Water and Energy Design and Supervision Works Sector resource, Addis Ababa
42. WEDSWS (2019) Groundwater resource assessment for areas of South Teru, Chifra and surroundings. Ethiopian Construction Design and Supervision Works Corporation, Water and Energy Design and Supervision Works Sector resource, Addis Ababa
43. Wolfenden E, Ebinger C, Yirgu G, Renne P, Kelley S (2005) Evolution of a volcanic rifted margin: Southern Red Sea, Ethiopia. Geol Soc Am Bull 117:846–864
44. Yitbarek A, Razack M, Ayenew T, Zemedagegnehu E, Azagegn T (2012) Hydrogeological and hydrochemical framework of Upper River basin, Ethiopia: With special emphasis on inter-basins groundwater transfer between Blue Nile and Awas Rivers. J Afr Earth Sci 65 (2012) 46-60. dio:10.1016/j.jafreasci.2012.01.002
45. Zwaan F, Corti G, Keir D, Sani F, (2019) A review of tectonic models for the rifted margin of Afar: implications for continental break-up and passive margin formation. J Afr Earth Sci. https://doi.org/10.1016/j.jafrearsci. 2019.103649.

46. Zwaan F, Corti G, Sani F, Keir D, Muluneh AA, Illsley-Kemp F, Papini M (2020) Structural analysis of the Western Afar Margin, East Africa: Evidence for multiphase rotational rifting. Tectonics, 39, e2019TC006043. https://dio.org/10.1029/2019TC006043

Figures

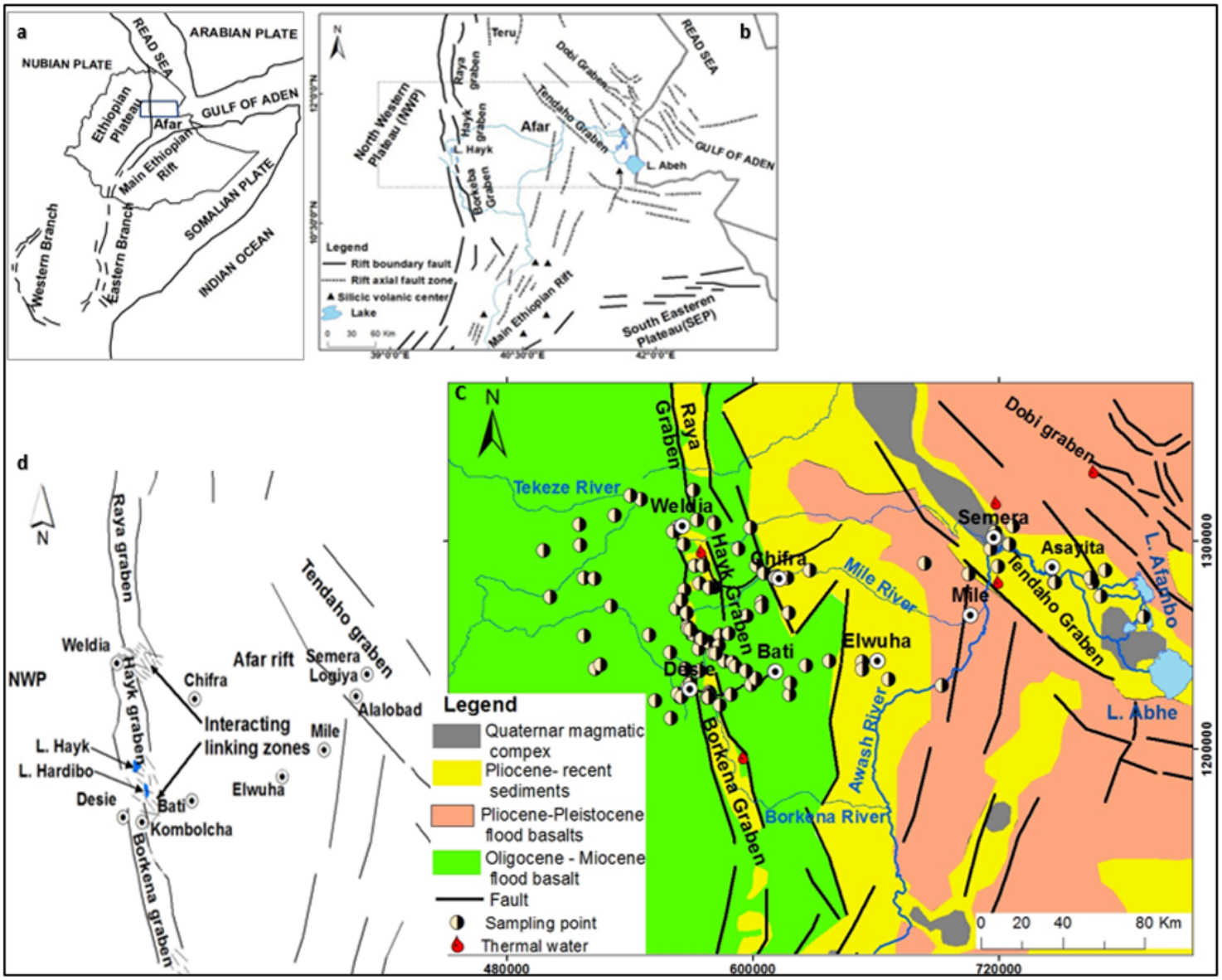

Figure 1

Map showing the location of the study area in relation to the East African Rift, the Red Sea and Gulf of Aden (a and b), the geology, major structural features and water sampling points (c), and the arrangement and orientations of the marginal grabens and the linkage zones in between them (d) (Geological and structural data GSE 2013)

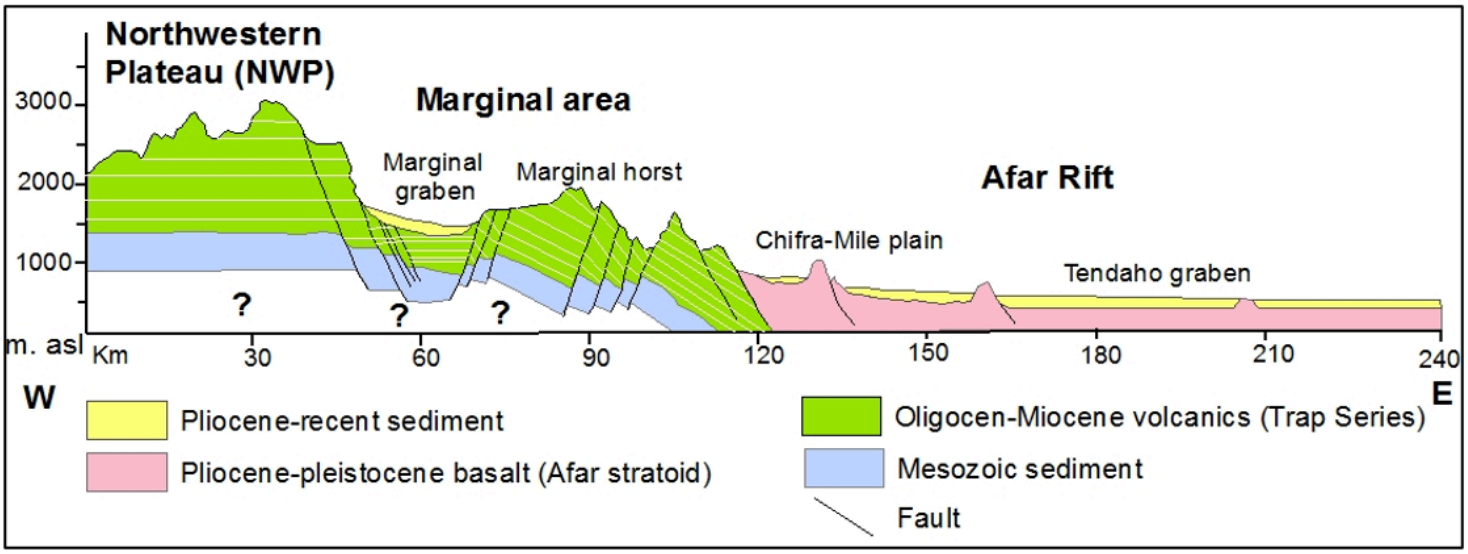

Figure 2

Schematic geological and geomorphological cross section across NWP and central Afar rift (Geological data Beyene and Abduselam 2005; GSE 2013)

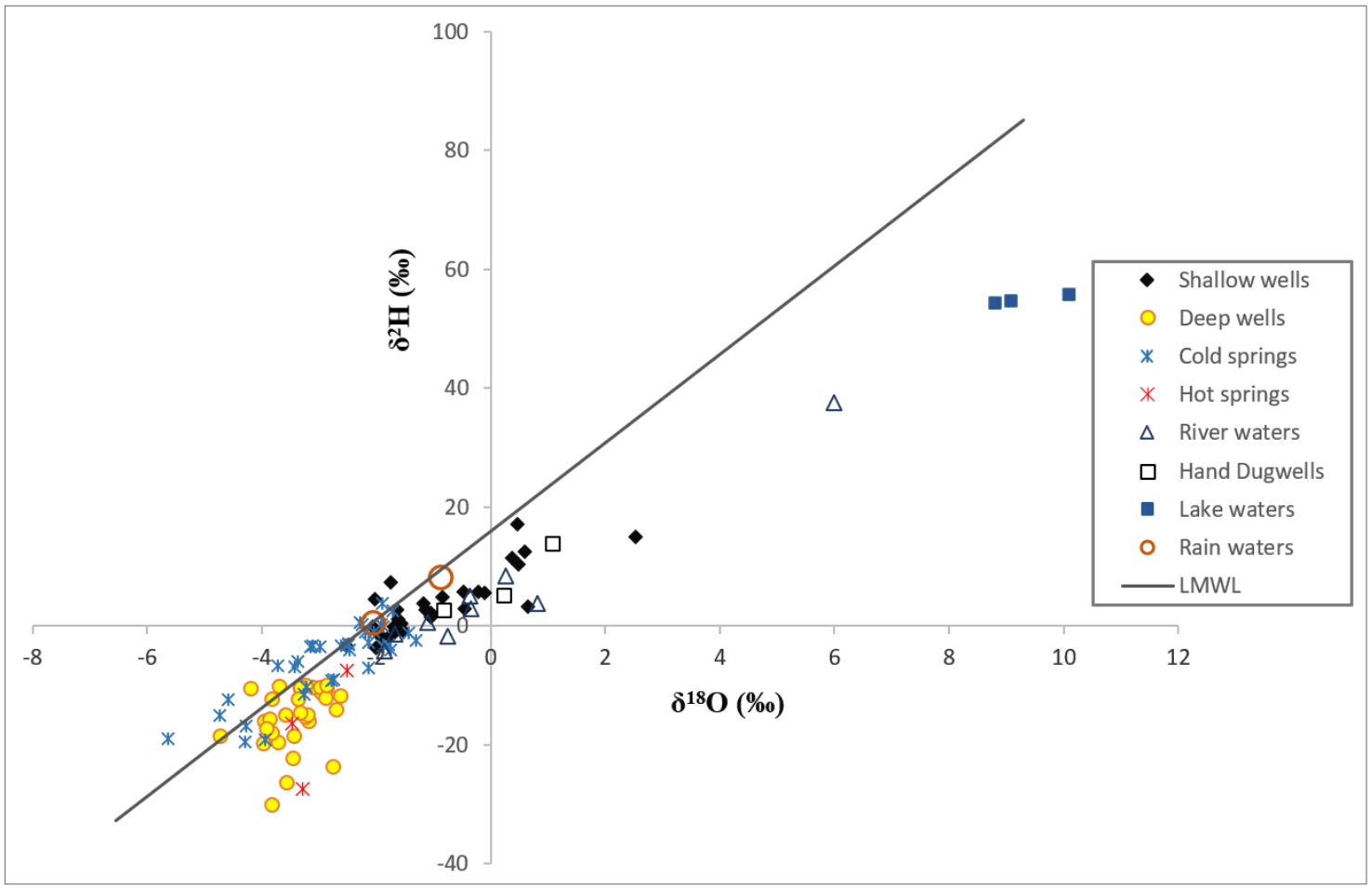

Figure 3

$\delta^{18}O$ versus $\delta^{2}H$ plots of all waters from NWP, Marginal garbens and Afar Rift floor plotted along with the LMWL of Addis Ababa rainfall IAEA station (1965 -2009) represented by a straight line equation $\delta D=7.659\ \delta^{18}O +11.8$

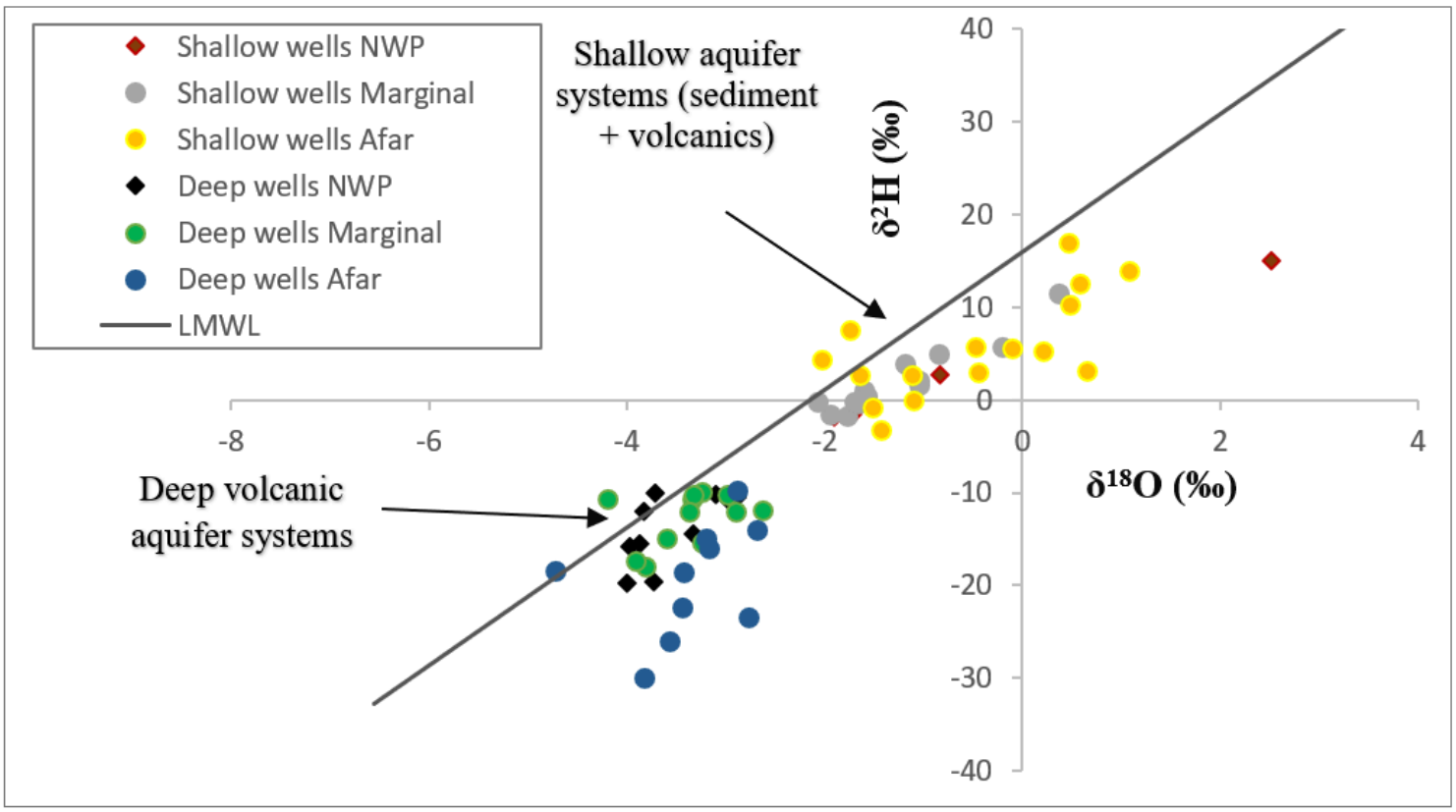

Figure 4

The $\delta^{18}O$ and $\delta^{2}H$ plots of waters from wells/boreholes in the NWP, Marginal area and the Afar rift alluvio-lacustrine sediment and volcanic Aquifers

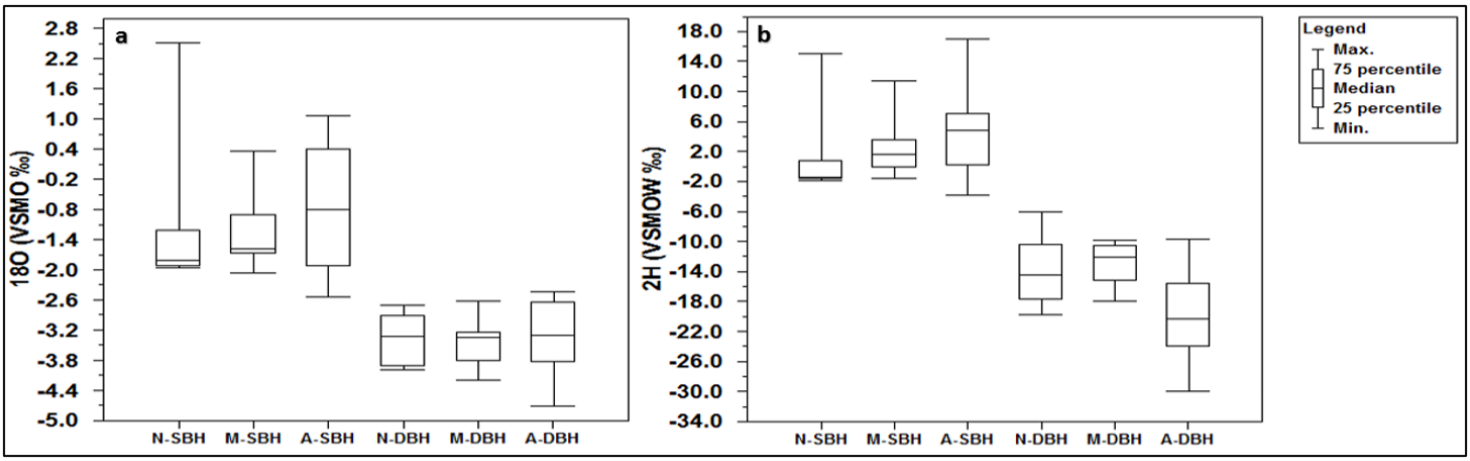

Figure 5

The variation of ^{18}O (a) and $\delta^{2}H$ (b) from the NWP to Afar rift (N-SBH=northwestern plateau shallow aquifers, M-SBH=marginal area shallow aquifers, A-SBH=afar rift shallow aquifers, N-DBH northwestern plateau deep aquifers, M-DBH= marginal area deep aquifers, A-DBH= afar rift deep aquifers)

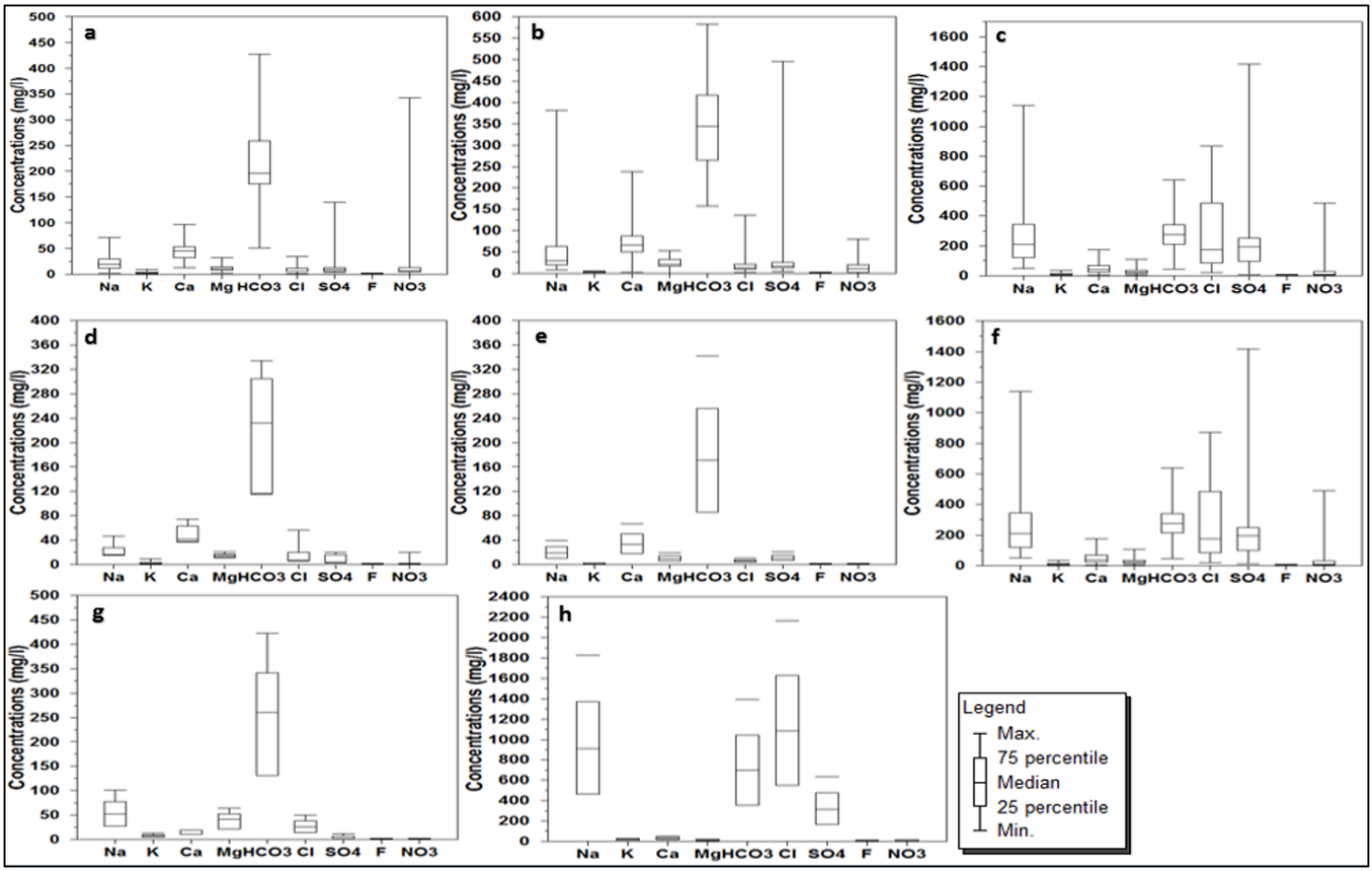

Figure 6

Composition of major elements in groundwater and surface waters. **a** NWP groundwaters; **b**marginal area groundwaters; **c** Afar rift groundwaters; **d** NWP Rivers; **e** Marginal area Rivers; **f** Afar rift rivers; **g** Marginal area lakes; **h** Afar rift lakes

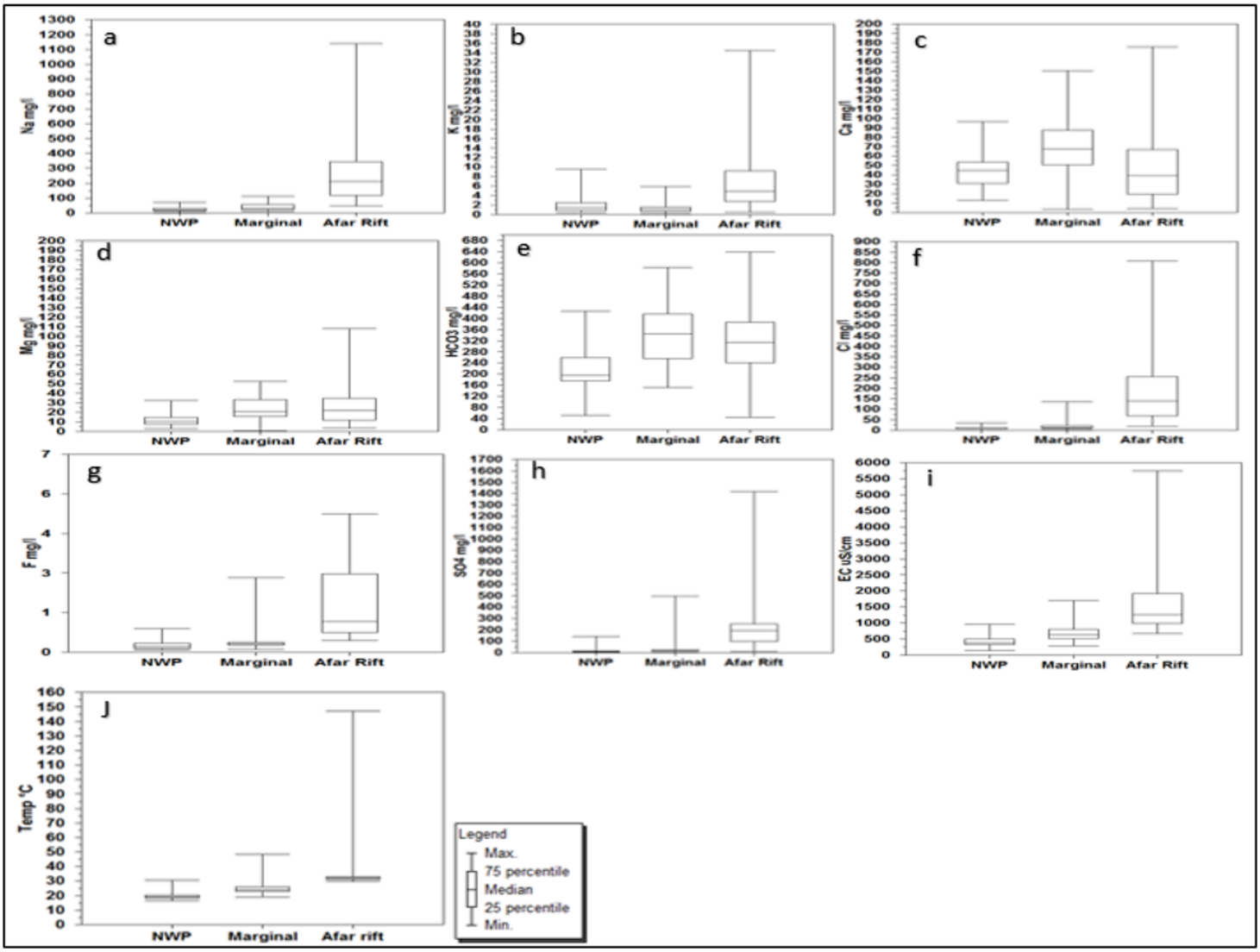

Figure 7

The variation of groundwater major ions, EC and T^0 from the NWP, across Marginal area to the Afar rift.

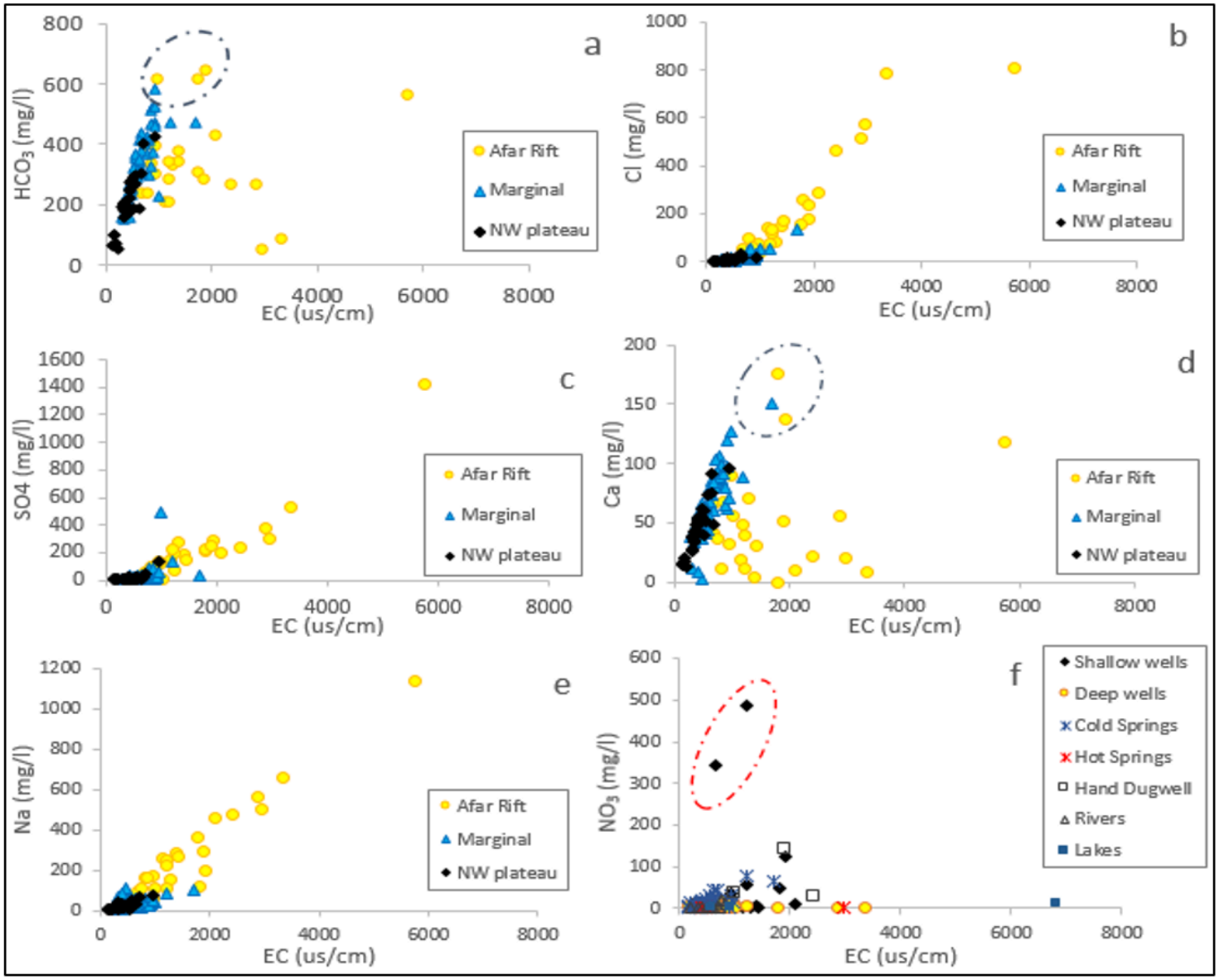

Figure 8

The relationship between EC and major ions in groundwaters of various location within the NWP, marginal grabens and the Afar rift

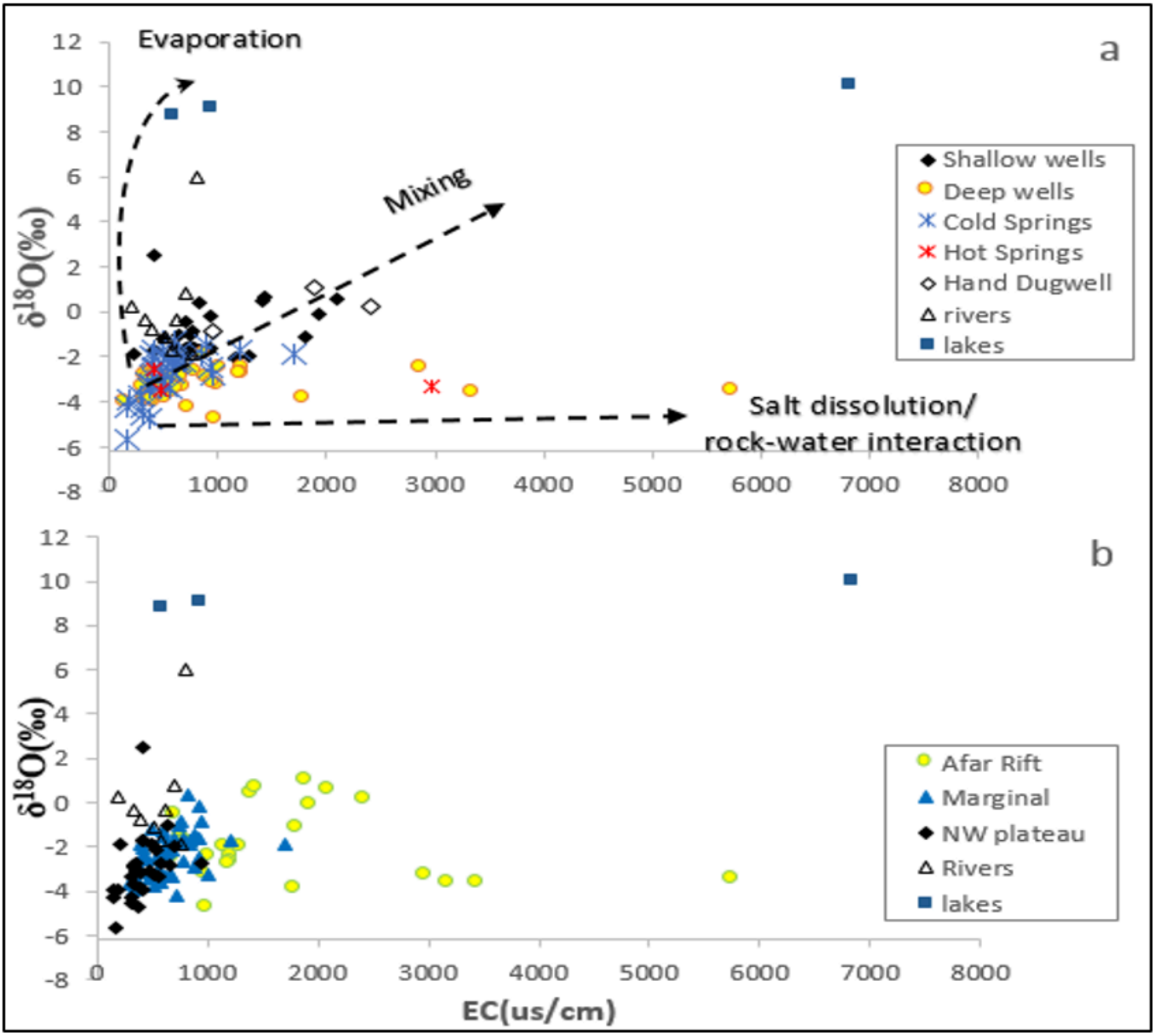

Figure 9

EC versus ^{18}O contents in surface waters, deep and shallow groundawters (a) compared with their spatial variations from the NWP, marginal area and the Afar rift (b)

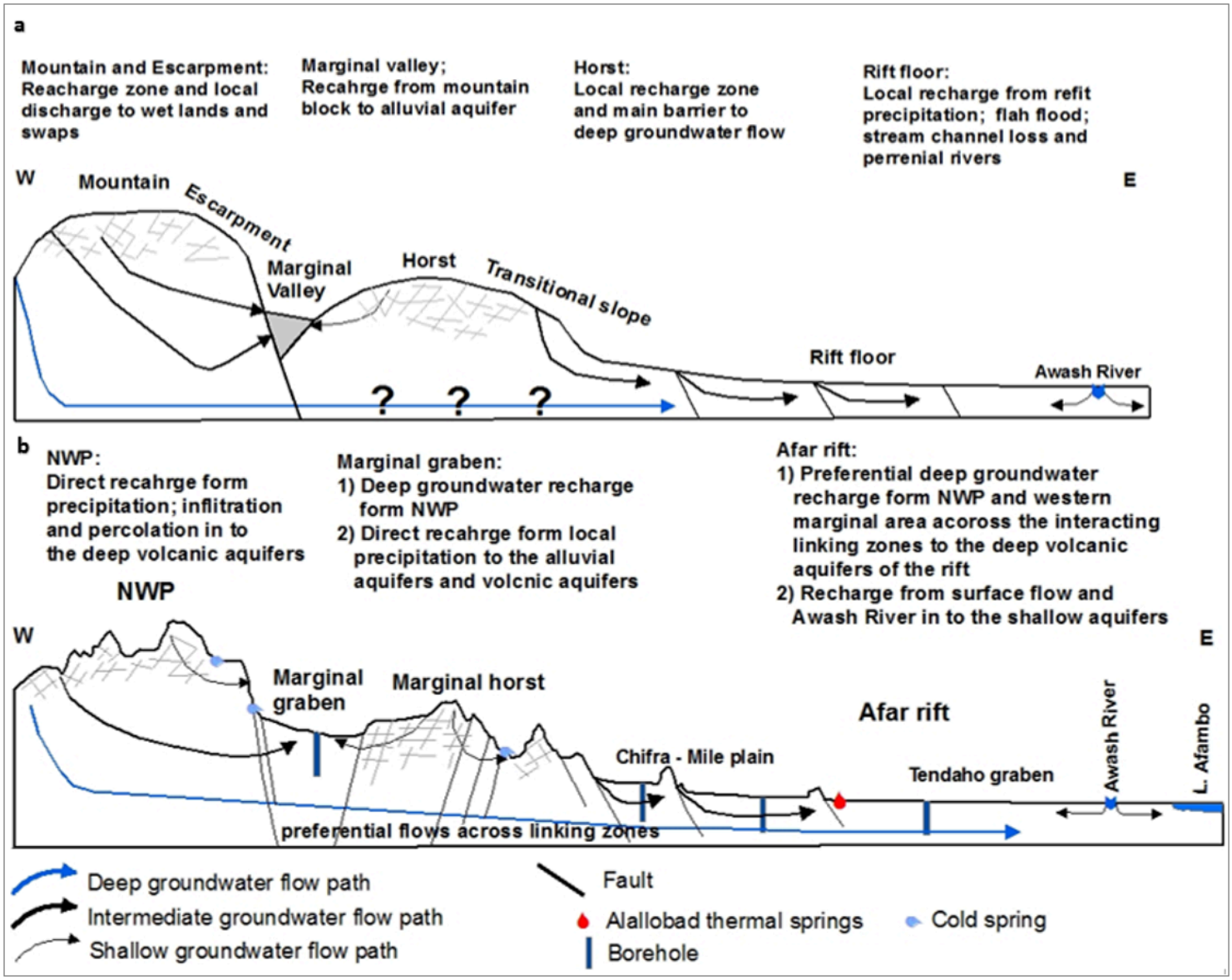

Figure 10

Schematic diagram of groundwater recharge and flow patterns (not to scale) representing the conceptual model of groundwater flow, **a** existing (after Kebede et al. 2007) and **b** this study

Supplementary Files

This is a list of supplementary files associated with this preprint. Click to download.

- SupplementaryTable1.docx